Hybrid Energy Harvesting System Based on Regenerative Braking System and Suspension Energy Harvesting for Middle Electric Vehicle

Kunagone Kiddee

Program in Electronics and Automation Systems Engineering, Faculty of Technical Education, Rajamangala University of Technology Thanyaburi. Rangsit-Nakhonnayok Rd. Klong6, Thanyaburi Pathum Thani

Corresponding Author. E-mail address: kkunagone@gmail.com

Received: 22 October 2020; Revised: 8 December 2020; Accepted: 14 December 2020
Published online: 25 December 2020

Abstract

This research proposed a hybrid energy harvesting system (HEHS) based on Suspension Energy Harvesting using a regenerative shock absorber (RSA) with SC/Battery hybrid energy storage system (SCB-HESS) based regenerative braking system (RBS) for the middle electric vehicle (MEV). In the regenerative braking mode, the artificial neural network (ANN)-based RBS control mechanism was utilized to optimize the switching scheme of the three-phase inverter and transferred the braking energy to be stored in the energy storage devices. Furthermore, a supercapacitor-based RSA is capable of harvesting the vehicular suspension-vibration energy and converting it into electrical energy to extend energy storage devices. The experimental total energy harvesting efficiency of the supercapacitor-based RSA ranges between 21.74% and 49.93%, with an average total efficiency of 31.93%. In addition, the research findings revealed that the proposed hybrid energy harvesting system based on SCB-HESS-based RBS with suspension energy harvesting using RSA enhanced the regeneration efficiency of 31.75% compared with SCB-HESS-based RBS MEVs.

Keywords: Electric Vehicle (EV), Brushless DC (BLDC) motor, Neural Network (NN), Regenerative Braking System (RBS), Supercapacitor, Suspension-vibration energy.

I. INTRODUCTION

Rapid economic growth and rising affluence contributes to an increase in private-car ownership, which consequently contributes to increased toxic vehicular emissions. At present, most battery electric vehicles are run on electrochemical batteries (i.e. the main energy storage system) [1]-[6]. However, electrochemical batteries suffer from a number of drawbacks, including high cost, short life cycle, limited driving range and low power density as well as subsequent diminished regenerative braking efficiency. The present state of energy harvesting that efforts to convert lost energy into an available form does not focus on the vehicle but on components instead [1], [4]. Energy harvesting technology has significant potential for the present automotive industry by improving vehicle energy efficiency and fuel economy. For electric vehicles technologies, regenerative braking energy, and the vehicular suspension-vibration energy are the main targets of energy harvesting [7]. Furthermore, a bulky energy storage system (ESS) containing multiple battery packs is required to meet the vehicle regenerative braking efficiency.

To overcome the drawbacks, a hybrid energy storage system (HESS) based on multiple battery and supercapacitors (SC) was utilized to improve vehicle acceleration and prolong the battery life span [3]. Different energy management strategies have been proposed in literature for optimal power split strategies in HESSs [1]–[6]. Majority of the prior work is proposed for fuel cell systems hybridized with SC and/or batteries. Similar energy management techniques can be adopted for battery/SC hybridization. Strategies that are based on heuristics or empiric experience can be easily implemented by rule-based control algorithms [4]–[6] or using fuzzy logic methods [1], [4]. The simple filter-based or frequency-based power split strategies have been implemented in [11] and [12].

For a conventional EV, a significant amount of energy is consumed in urban driving cycles by braking [1], [2]. To improve the performance of EVs, the regenerative braking system has been developed. It utilizes the electric motor, providing negative torque to converting kinetic energy to electrical energy for recharging the energy storage devices. The dissipation of kinetic energy during braking, by an electric vehicle can be recovered advantageously by controlling the power electronics for total energy management onboard the vehicle. Therefore, regenerative braking is an efficient technology to improve the efficiency of electric vehicles. Various attempts to satisfy the control performance needs for regenerative braking have been presented in the literature, such as rule-based strategies [5]-[6], PID control strategies [3]–[5], and neural network approaches [4]. in the regenerative braking condition, the DC-link voltage is boosted. Hence, the ANN controller-based RBS program transferred the braking energy to store in the SC. [5]-[6]. Specifically, the battery/SC HESS scheme utilizes the high power density of an SC and the high energy density of a battery. Nevertheless, a high-power electronic interface, e.g. the bidirectional DC/DC converter, is required to connect the battery and the SC, rendering it cost-ineffective [1]-[6]. Moreover, the high-power electronic interface induces the power dissipation and the subsequent diminished regenerative braking efficiency [6].

In practice, shock-absorber vibration energy corresponds to road roughness and vehicle speed [7], [8], and [10], experimented with the hydraulic damper with a permanent-magnet synchronous machine and variable resistors; Despite extensive studies focused on regenerative shock absorbers (i.e. electromagnetic, hydraulic and mechanical schemes) [9]-[15] and [18], The electricity produced by the generator is stored in supercapacitors to charge the battery and extend the

range of EVs. The mechanical properties of the full-scaled fabricated prototype were studied by utilizing a mechanical testing and sensing fixture. An average power output of 3.701 W in 1Hz-3 mm sinusoidal vibration input and a peak efficiency of 51.1% and average efficiency of 36.4% were achieved in a bench test [14]-[16].

Several designs of energy harvesting suspension systems have been presented and optimized in order to ensure an improved performance for different applications. Moreover, regenerative braking has already been available and applied to hybrid and electric vehicles commercially. However, both the energy harvesting suspension systems and regenerative braking technology is still under continuous development. It can be concluded through studies that both energy harvesting methods have limitations such as total weight increases, extra space requirements, system losses, efficiency losses, costs, etc. In this respect, optimizations continue for more light weighted designs with choosing the more suitable material selection, power electronic interface, suitable switching control and dimensional designs [7], [17].

Specifically, this research experiments with the proposed a HEHS based on suspension energy harvesting using regenerative shock absorber (RSA). The proposed RSA composed of three main parts; the suspension vibration energy, conversion mechanism and energy storage modules with SC/battery Hybrid Energy Storage System (SCB-HESS) based RBS, in the regenerative braking condition, the DC-link voltage is boosted. Hence, the ANN-based RBS program with suitable switching pattern of three phase inverter transferred the braking energy to store in the SC, both the energy harvesting was utilized to extend the battery life and the driving range for MEV.

II. THE SCB-HESS REGENERATIVE MODE

In the SC-enabled regenerative braking mode, the DC-link voltage is boosted and power diode becomes forward-biased a boost circuit of the three-phase inverter can be formed. High sides of the switches of the half-bridge are turned off and the low sides of the switches are pulse width modulated [6]. The regenerative braking energy is then transferred and stored in the SC module (Figure 1 b) Conventionally, an additional buck-boost DC/DC converter is deployed to transfer the braking energy to the SC, as shown in Figure 1, (a) SC-enabled regenerative braking mode by regenerative shock absorbers, and (b) SC-enabled regenerative braking by RBS.

III. THE CONVERSION MECHANISM

The conversion mechanism converts the bidirectional between the inner and outer cylinders in linear motion (up-down movements) into a unidirectional rotation to drive the generator shaft. Figure 2(a) illustrates the prototype and 3D model of the RSA, consisting of two cylinders, bevel gears, overrunning clutches, rack-pinions, a shaft and internal gear as shown in Figure 2(b) [15].

In Figure 2(b), the shaft with two pinions is assembled without being stationary. The unidirectional overrunning clutches (CSK-PP type) are fitted to the shaft and fixed into the pinions [15].

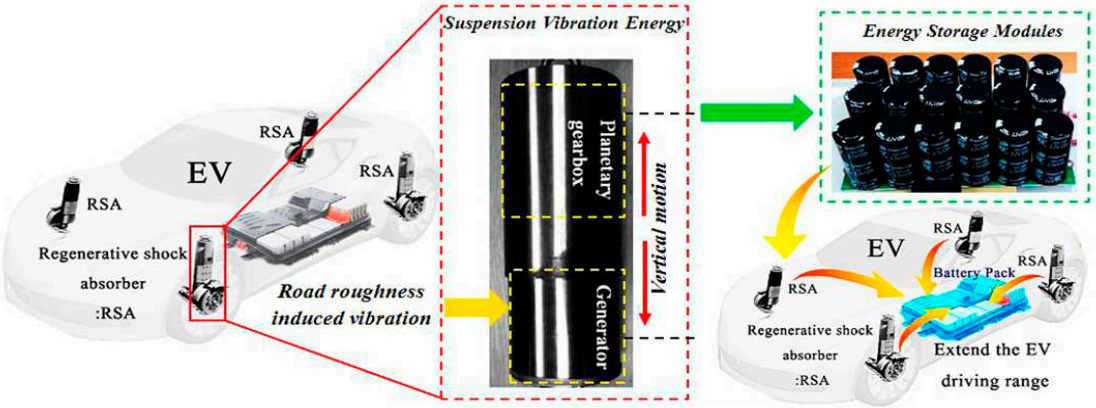

(a)

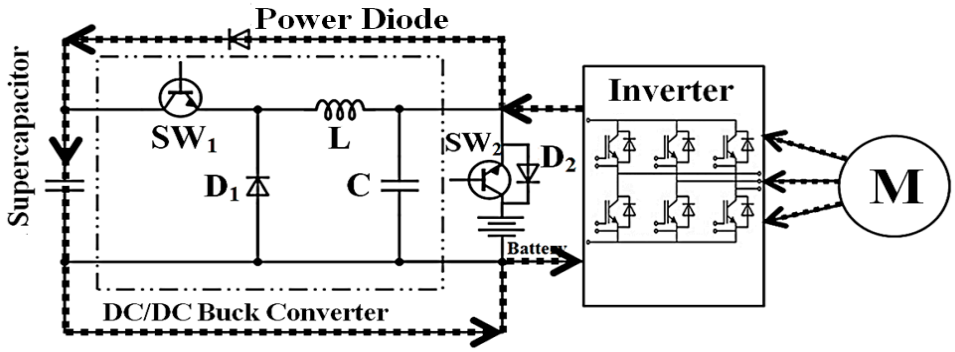

(b)

Figure 1 The conversion mechanism of the proposed system (a) SC-enabled regenerative braking mode by regenerative shock absorbers (b) SC-enabled regenerative braking by RBS

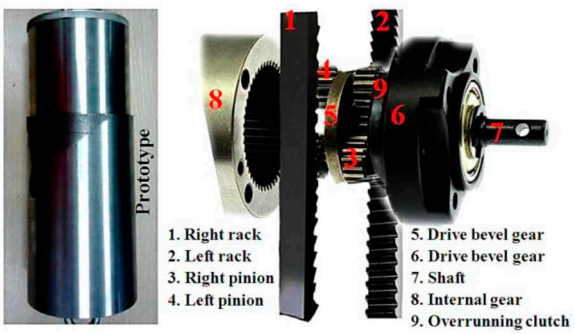

(a) (b)

Figure 2 The prototype and 3D model of the RSA: (a) outer, and (b) inner structure

Upon vibration, the alternating pattern of movement between the inner and outer cylinders in linear motion induces the upward and downward movements of the racks. The racks then transmit the vertical movements to the left-right pinions. Given the rack and pinion assembly, the two pinions rotate in directions opposite to each other [15]. The dual overrunning clutches alternately engage and disengage the shaft (i.e. if one overrunning clutch engages, the other disengages), This, results in the unidirectional rotation motion of an output shaft, independent of the movement of the racks, as shown in Figure 3.

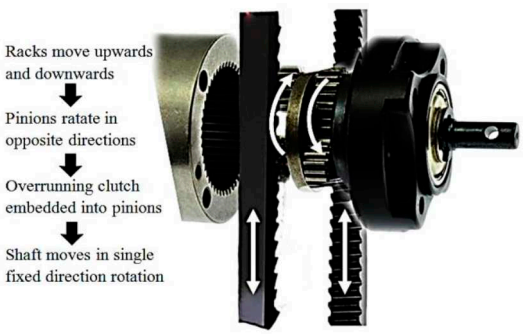

Figure 3 The conversion mechanism with bidirectional linear motion into a unidirectional rotation

IV. SYSTEM POWER ANALYSIS

In this study, the conduction and switching losses of the dc–dc buck converter is considered for buck mode. The dc–dc buck converter power electronic interface conduction losses of the high-side switch is computed as

$$P_{on,H} = I_{out}^2 \times R_{on,H} \times \frac{V_{out}}{V_{in}} \quad (1)$$

The dc–dc converter conduction losses of the low-side IGBT can be written as

$$P_{on,L} = I_{out}^2 \times R_{on,L} \times \left(1 - \frac{V_{out}}{V_{in}}\right) \quad (2)$$

where V_{in} is the input voltage, and V_{out} is the output voltage. $P_{on,H}$ is the high-side IGBT on resistance, $P_{on,L}$ is the low-side IGBT on resistance.

The switching losses of dc–dc converter can be expressed as:

$$P_{sw,loss} = f_s \begin{pmatrix} \frac{1}{2} V_C |I_L| (t_r + t_f) + \frac{1}{2} V_C^2 C_{oss} \\ + Q_{charge} V_G + V_C Q_{rr} \end{pmatrix} \quad (3)$$

C_{oss} is the output capacitance of IGBT. Q_{charge} is the gate charge due to charging the gate capacitance by gate voltage. Q_{rr} is the reverse recovery charge. V_G is the gate voltage. t_r and t_f are the rise-time and fall-time transitions of IGBTs during switching periods.

The total power losses in HESS are the sum of power losses in the dc–dc buck converter, inverter, motor, during braking and the SC/battery as

$$P_{HESS,loss} = P_{on,H} + P_{on,L} + P_{sw,loss} + P_{Diode} + P_{Inv.Mot,loss} + P_{brake} + I_{SC}^2 R_{SC} + I_{batt}^2 \quad (4)$$

where $P_{Inv.Mot,loss}$ is the power of losses at power level (P). Since the total power loss is obtained, the efficiency can be calculated with the following equation

$$\eta = \frac{V_{OUT} \times I_{OUT}}{(V_{OUT} \times I_{OUT}) + P_{HESS,loss}} \quad (5)$$

where V_{OUT} is the output voltage. I_{OUT} is the output current.

This part investigates the effects of the RSA scheme parameters (e.g. damping force, excitation force) on the output power efficiency. Specifically, the damping force (F_d) of the RSA can be expressed as

$$F_d = F = m_{eq}\ddot{x} + \dot{C}_L = m_c + 2m_r + \frac{\frac{J_g}{i^2} + J_{pg} + J_b + J_s + 2J_p}{r^2} \times \ddot{x} + \frac{1.5 \times k_e^2}{\beta_g \beta_{pg} \beta_b \beta_{rp} i^2 r^2 (R_e + R_i)} \times \dot{x} \quad (6)$$

where F_d is the damping force, F is the excitation force, x is the excitation speed, and $\beta_g, \beta_{pg}, \beta_b, \beta_{rp}$ are the efficiency of the generator, planetary gearbox, bevel gear and rack-pinion, respectively. m_c and m_r are the mass of the outer cylinder and the rack, while, $J_g, J_{pg}, J_b, J_s, J_p$ are the inertia of the generator, planetary gearbox, bevel gear, shaft and pinion respectively. k_e is the rotary damping coefficient, R_i is the Internal resistor of each phase of the generator charging circuit, R_e is external resistors, r is the radius of the pinion, i is the planetary gear ratio and C_L is the linear damping coefficient[15].

The mechanical efficiency (β_m) of the RSA is expressed as

$$\beta_m = \beta_g \beta_{pg} \beta_b \beta_{rp} \quad (7)$$

Substituting (2) into (1) yields

$$\beta_m P_{input} = P_E \quad (8)$$

where P_E is the electrical power, which comprises the fragment charge captured ($P_{captured}$) and the fragment lost to the internal resistance (P_{lost}) of the generator, which can be calculated as:

$$P_E = P_{captured} + P_{lost} \quad (9)$$

Thus, the electrical efficiency of the RSA is calculated by

$$\beta_e = \frac{P_{captured}}{P_{captured} + P_{lost}} \quad (10)$$

The linear damping coefficient can be calculated as follows:

$$C_L = \frac{\Delta W}{\pi \omega A^2} \quad (11)$$

where C_L is the linear damping coefficient, ΔW is the mechanical work input of the RSA, ω and A are the frequency and amplitude of the sinusoidal vibration, respectively.

V. DESIGN OF BEACH TEST EXPERIMENTAL

In this research, a 20 kW BLDC motor [6] was selected since it has higher power to weight ratio efficiency compared to other motors. For example, in comparison to an induction motor, the 20 kW BLDC motor has a weight of 40.5 kg., which is lighter than the 20 kW BLDC motor which has a weight of 102.5 kg. For this reason, it is lighter, smaller, and more suitable for installation in middle electric vehicles with a weight range of 400-800 kg and suitable for an average running speed of 30-85 km/h. Details for the beach test experimental are shown in Figure 4.

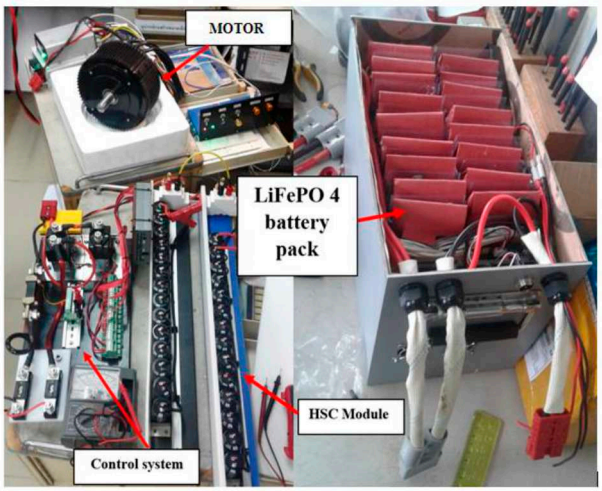

Figure 4 Test bench experiment of regenerative braking system.

VI. EXPERIMENTAL RESULTS AND DISCUSSION

Figure 5 shows the simulation and experiments of the relationship between speed and the time spent using the braking range of 9.26 seconds at a pre-braking speed of 34.84 km/h to evaluate the supercapacitor pressure before/after braking which results from the simulation found that during the previous period and after braking for 9.26 seconds at an average speed of 34.15 km/h before the braking speed, SC voltage is increased after braking to 5.8 v, where Table I shows the experimental results, kinetic energy before braking and the energy stored after braking at the speed before braking, averaging 9.41 m/s at the time of braking at 9 seconds. The energy stored after braking averages at 3,215.02 joules. The kinetic energy that occurs before braking averages at 27,250.90 joules.

The RSA bench-test experiments carried out subject to sinusoidal vibration given variable frequencies (2.0, 2.5, 3.0, 3.5 Hz) and amplitudes (3, 6, 9 mm) for the force-displacement loops. The experimental platform of the RSA prototype using HS-5042-AF2 electronic shock absorber testing system and a UTD2102CEX-EDU digital oscilloscope to record the voltage signals from the generator. Due to the dimensional limitations, the maximum amplitude of the prototype RSA is 9 mm.

Table 1 Experimental and Simulation Specifications

Set	Speed before braking (m/s)	Total kinetic energy before braking(J)	Duration of braking (s)	Energy recovered (J)
1	9.60	27,490.43	9.24	2,240.31
2	9.71	28,523.75	9.28	2,811.49
3	9.55	27,233.27	9.24	3,286.39
4	9.59	27,531.91	9.32	3,491.02
5	9.52	27,438.08	9.25	4,127.75

The efficiency of the proposed method can be evaluated by comparing the SOC of the hybrid energy storage device. (SC and batteries) during the driving cycle of MEV, Figure 5 shows the comparison of simulations and experiments for the charge status of the SC and battery under 2 conditions: the system recovers braking using SC with the charge status of the SC and the battery starting at 87.2% and 82.6%. The system recovers braking using battery with the SOC of SC and batteries starting at capacitors 96.1% and 85.5%.

The multi-layer feed-forward ANN provide satisfactory ANN capability in this proposed scheme. The inputs comprise the vehicle speed, states of charge (SOC) of the SC and the battery, and the number of brake situation per drive cycle. The regenerative braking force of the front wheel are the outputs of the ANN algorithmic scheme. Five neurons in hidden layer are analyzed. Meanwhile, the hidden layer of the algorithmic scheme consists of five neurons whose activation functions are of sigmoid function [6].

The artificial neural network (ANN)-based RBS control mechanism was utilized to optimize the switching scheme of the RBS's three-phase inverter. In the regenerative braking mode, the ANN-based SC/battery RBS transferred the braking energy to be stored in the SC [6].

In the first case, the initial SOC value of the SC and the battery are set at 80.2% and 82.4% respectively. Therefore, the SC voltage is still far from the safety threshold of 93%, braking with the battery will not be activated. Consequently, there will be only SC used to store energy from braking in this case. With the SC status and battery in this case, Figure 6 shows the second case of braking, in which the SOC of the SC is set to an initial value of 96.2%, in this case, since the capacitor status (SOC) of the capacitor exceeds the set safety threshold.

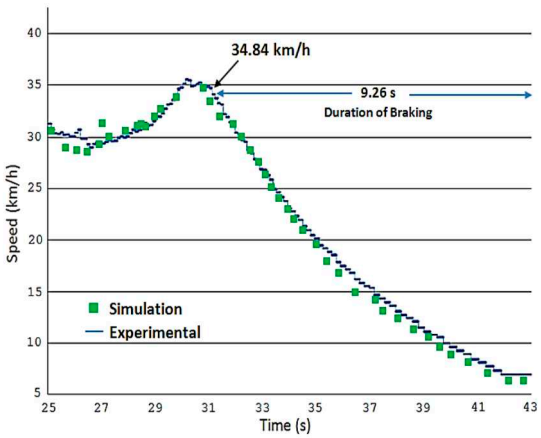

Figure 5 The simulation and experiments of the speed and time spent using the braking range of 9.26 seconds.

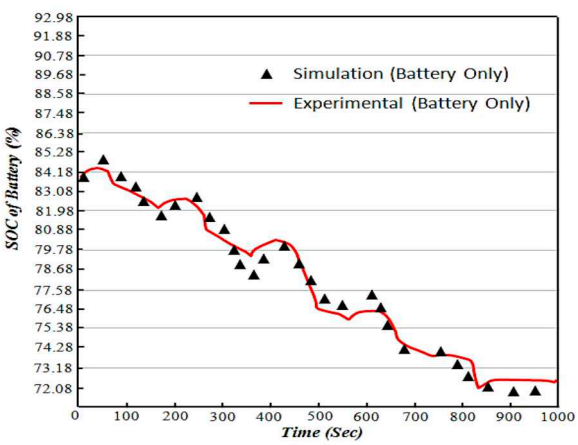

Figure 6 The initial SOC of 83.2% (Battery)

Table 2 tabulates the optimal simulation parameters of the RSA scheme. The RSA scheme was simulated using MATLAB based sinusoidal vibration under variable frequencies (2.0,2.5,3.0, 3.5 Hz) and amplitudes (3, 6, 9 mm) for the force-displacement loops. The sinusoidal vibration (x) function can be expressed as, where x is the sinusoidal vibration, t is the period time of frequency, A and ω are the amplitude and frequency of the sinusoidal vibration, respectively.

Figures 7(a)-(c) illustrate the simulated force-displacement loops of the proposed RSA scheme associated with 3, 6 and 9 mm amplitudes, given the frequencies of 2.0,2.5, 3.0, 3.5 Hz. The simulation results indicated that the regenerative shock absorber satisfied the requirements for conventional shock absorbers, particularly terms of in damping and elasticity [10]. The orientation of the force-displacement loops is non-horizontal and oblong-shaped, while the mass inertia is related to the negative slope. In addition, the ideal force-displacement loops could be achieved with the optimal simulation parameters [10], [11]

The simulation results also revealed that the vibrational frequency is positively correlated to the force-displacement loop slope, given 3, 6, 9 mm amplitudes. In other words, the loop slope increases with an increase in the excitation frequency. The non-horizontal loops are attributable to the masses of the outer cylinder (m_c) and the rack (m_r) as well as the inertia of the moving parts, i.e. the pinions, shaft, bevel gears, planetary gearbox and generator, as estimated by Eq. (1). By comparison, the simulated mechanical work input of the RSA (ΔW) (i.e. inner-loop area) increases with an increase in amplitude (3, 6, 9 mm), given the same excitation frequency.

Table 2 Experimental Optimal Simulation Parameters of the RSA

Parameter	Value
Pinion inertia J_p	*32.275 kg mm*^{2}
Shaft inertia J_s	*3.251 kg mm*^{2}
Bevel gear inertia J_b	*4.811 kg mm*^{2}
Planetary gearbox inertia J_{pg}	*0.22 kg cm*^{2}
Rotor inertia of generator J_g	*0.5 kg cm*^{2}
The mass of outer cylinder m_c	*3.401 kg*
The mass of rack m_r	*0.197 kg*
The rotary damping coefficient k_e	*0.0512 V s/rad*
the planetary gearbox ratio i	*1:35*

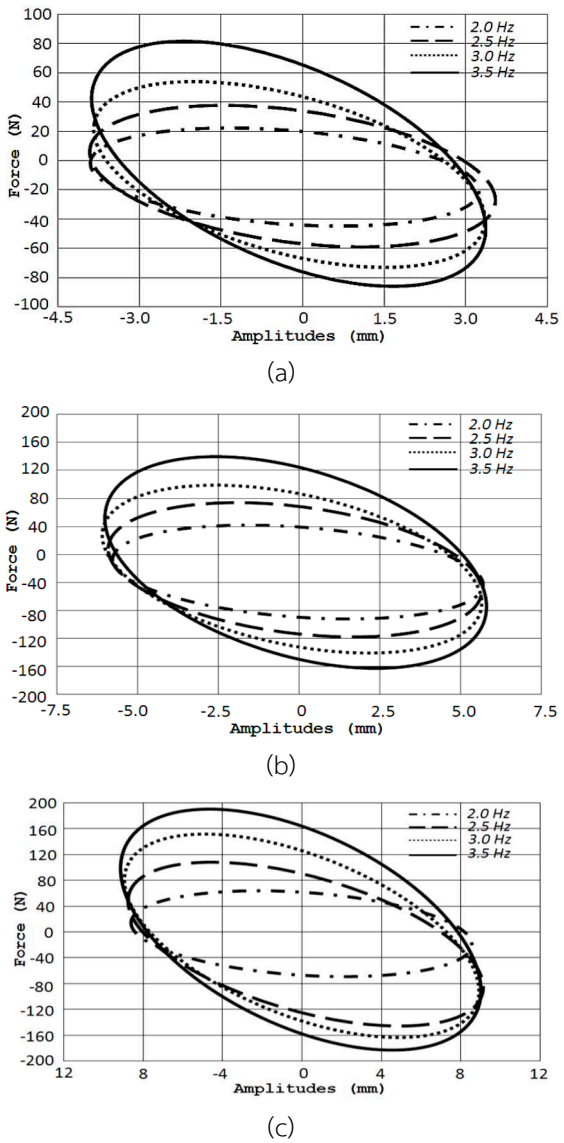

Figure 7 The simulated force-displacement loops under the frequencies of 2.0, 2.5, 3.0, 3.5Hz given the amplitude of: (a) 3 mm, (b) 6 mm and (c) 9 mm

Figure 8 illustrates the 9 mm-amplitude experimental force-displacement loops of the RSA scheme, given the frequencies of 2.0, 2.5, 3.0, 3.5 Hz. The inner-loop area represents the mechanical work input (ΔW) of the RSA.

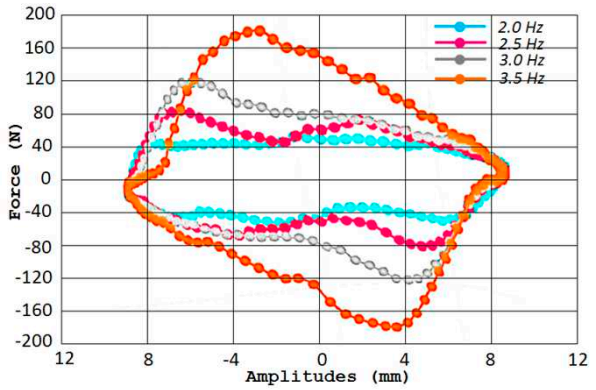

Figure 8 The experimental (bench test) force-displacement loops under frequencies of 2.0, 2.5, 3.0, 3.5Hz given amplitude of 9 mm

The average experimental linear damping coefficient (*CL*) is 1731.4 Ns/m, given 9 mm amplitudes. The experimental result closely resembles the calculated result of 1811.4 N s/m, calculated by (11).

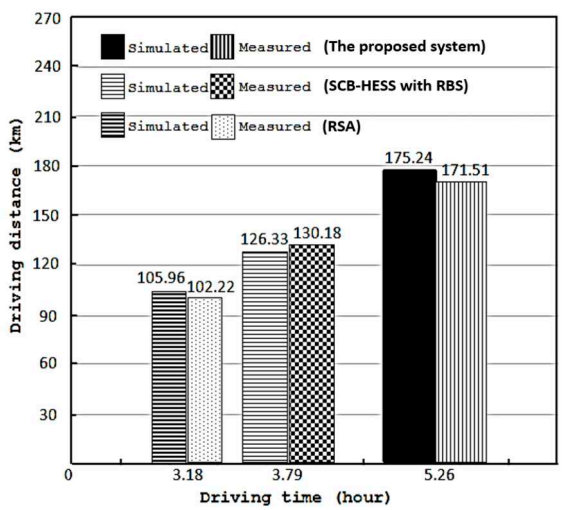

Figure 9 The driving range of the EV with RSA only, with the SCB-HESS with RBS only, with the proposed system (RSA with the SCB-HESS-based RBS)

Figure 9 compares the driving ranges and duration (drive cycle) of the EV without the RSA only, with SCB-HESS-based RBS, with the proposed system, given that one drive cycle is 8140.41 m with a total travelling time of 882.10 seconds. In the absence of the RSA only, the vehicle could travel 105.96 km (13 cycles) while, under the SCB-HESS-based RBS condition, the distance travelled by the EV was 126.33 km (15.5 cycles). Meanwhile, the distance logged by the vehicle with proposed system was 175.24 km (21.5 cycles), an increase of 48.91 km (6 cycles) compared to that of the RSA only vehicle.

VII. CONCLUSION

In this paper, a hybrid energy harvesting system was proposed based on a regenerative braking system and Suspension Energy Harvesting using Mechanical Regenerative Shock Absorber with SCB-HESS-based RBS for middle electric vehicles (MEV). In the regenerative braking mode, the DC-link voltage is boosted, and ANN-based RBS program transfers the braking energy to store in the energy storage devices.

In this study, experimental were carried out for an RSA prototype fabricated and bench-tested subject to sinusoidal vibration. The experimental RSA total efficiency (θ) was in the range of 21.74% -49.93%, with an average total efficiency of 31.93%. The total efficiency was positively correlated with the vibrational frequency and amplitude. The maximum total efficiency of 63.22% was achieved at 3.5 Hz frequency and 9 mm amplitude, to comparatively assess the performance of the proposed hybrid energy harvesting system, the simulations were carried out under the NYCC drive cycle. The results showed that the regeneration efficiency was improved about 31.75% in comparison with SCB-HESS-based RBS.

The proposed SCB-HESS-based RBS with suspension energy harvesting is capable of harvesting the braking

energy and the suspension vibration energy used for renewable energy applications to extend the battery life and the EV driving range.

REFERENCES

[1] J. Shen and A. Khaligh, "A supervisory energy management control strategy in a battery/ultracapacitor hybrid energy storage system," *IEEE Transactions on Transportation Electrification,* vol. 1, no. 3, pp. 223-231, Oct. 2015.

[2] A. Santucci, A. Sorniotti, and C. Lekakou, "Power split strategies for hybrid energy storage systems for vehicular applications," *Journal of Power Sources*, vol. 258, pp. 395–407, Jul. 2014.

[3] S. Dusmez and A. Khaligh, "A supervisory power-splitting approach for a new ultracapacitor–Battery vehicle deploying two propulsion machines," *IEEE Transactions on Industrial Informatics,* vol. 10, no. 3, pp. 1960–1971, Aug. 2014.

[4] M. Wlas, Z. Krzeminski, J. Guzinski, H. A. Rub, and H. A. Toliyat, "Artificial-neural-network-based sensorless nonlinear control of induction motors," *IEEE Transactions on Energy Conversion,* vol. 20, No. 3, pp. 520–528, Sep. 2005.

[5] A. Kuperman, I. Aharon, S. Malki, and A. Kara, "Design of a semiactive battery-ultracapacitor hybrid energy source," *IEEE Transactions on Power Electronics,* vol. 28, no. 2, pp. 806-815, Feb. 2013.

[6] X. Nian, F. Peng, and H. Zhang, "Regenerative braking system of electric vehicle driven by brushless DC motor," *IEEE Transactions on Industrial Electronics,* vol. 61, no. 10, pp. 5798-5808, Jan. 2014.

[7] U. Aksu and R. Halicioglu, "A review study on energy harvesting systems for vehicles," *Tehnički Glasnik*, vol. 12 no. 4, pp. 251-259, Dec. 2018, doi: 10.31803/tg-20180210153816.

[8] M. A. A. Abdelkareem, L. Xu, M. K. A. Ali, A. Elagouz, J. Mi, S. Guo, Y. Liu, and L. Zuo, "Vibration energy harvesting in automotive suspension system: A detailed review," *Applied Energy,* vol. 229, pp. 672-699, Nov. 2018.

[9] H. Wang, A. Jasim, and X. Chen, "Energy harvesting technologies in roadway and bridge for different applications-a comprehensive review," *Applied Energy,* vol. 212, pp. 1083–1094, Feb. 2018.

[10] C. Wei and X. Jing, "A comprehensive review on vibration energy harvesting: Modelling and realization," *Renewable and Sustainable Energy Reviews,* vol. 74, pp. 1–18, Jul. 2017.

[11] W. Salman, L. Qi, X. Zhu, H. Pan, X. Zhang, S. Bano, Z. Zhang, and Y. Yuan, "A high-efficiency energy regenerative shock absorber using helical gears for powering low-wattage electrical device of electric vehicles," *Energy,* vol. 159, pp. 361-372, Sep. 2018.

[12] A. Emadi, Y. J. Lee, and K. Rajashekara, "Power electronics and motor drives in electric, hybrid electric, and plug-in hybrid electric vehicles," *IEEE Transactions on Industrial Electronics,* vol. 55, no. 6, pp. 2237–2245, Jun. 2008.

[13] L. W. Ching, L. C. Liang, H. P. Min, and W. M. Tzong, "Realization of anti-lock braking strategy for electric scooters," *IEEE Transactions on Industrial Electronics,* vol. 61, no. 6, pp. 2826–2833, Jun. 2014.

[14] Z. Fang, X. Guo, L. Xu, and H. Zhang, "Experimental study of damping and energy regeneration characteristics of a hydraulic electromagnetic shock absorber," *Advances in Mechanical Engineering,* vol. 3, pp. 1-9, May 2013, doi: 10.1155/2013/943528.

[15] Z. Zhang, X. Zhang, W. Chen, Y. Rasim, W. Salman, H. Pan, Y. Yuan, and C. Wang, "A high-efficiency energy regenerative shock absorber using supercapacitors for renewable energy applications in range extended electric vehicle," *Applied Energy,* vol. 178, pp. 177-188, Sep. 2016.

[16] Z. Wang, T. Zhang, and Z. Zhang, "A high-efficiency regenerative shock absorber considering twin ball screws transmissions for application in range-extended electric vehicles," *Energy and Built Environment,* vol. 1, no. 1, pp. 36-49, Jan. 2020.

[17] Y. Zhang, X. Zhanga, M. Zhana, K. Guoa, F. Zhao, and Z. Liu, "Study on a novel hydraulic pumping regenerative suspension for vehicles," *Journal of the Franklin Institute,* vol. 352, no. 2, pp. 485-499, Feb. 2015, doi: 10.1016/j.jfranklin.2014.06.00.

[18] Z. Zhao, T. Wang, B. Zhang, and J. Shi, "Energy Harvesting from Vehicle Suspension System by Piezoelectric Harvester," *Journal of the Mathematical Problems in Engineering,* vol. 2019, 2019, Art. no. 1086983, doi: 10.1155/2019/1086983.